

## Basic Research on Flexural Damage of RC Piers Having Cut-off Rebars



Hisako Kobayashi\*



Kaoru Kobayashi\*\*



Mitsuru Shimizu\*\*

Some reinforced concrete (RC) piers have cut-offs where the number of rebars in the longitudinal direction are reduced at an intermediate section of the pier frame. Those cut-offs are created by shortening some longitudinal rebars and locating those rebars up to the middle of the pier frame. Since the shortened rebars are anchored to the concrete and generate tensile stress, they cause bond deterioration, often leading to damage at an earthquake. In this research, we carried out cyclic loading tests using specimens that had cut-off rebars of specifications where flexural damage is predominant and clarified four damage modes. Examining the cyclic loading test results, we propose a method of identifying the flexural damage mode of an RC pier having cut-off rebars based on a comparison of flexural capacity performance at the rebar cut-off point and the anchorage strength of the cut-off rebars above the cross-section height (D) of the pier.

●Keywords: Rebar cut-off point, RC pier, Flexural damage, Cyclic loading test

### 1 Introduction

Some reinforced concrete (RC) piers have cut-offs where the number of rebars in the longitudinal direction are reduced according to the cross-sectional force. With such piers, the cover concrete can spall in a large earthquake (Photo 1). Usually RC piers receive damage at their bases. Thus, for RC piers set in a river or those with deep-set bases, it is expected that recovery work after an earthquake would require huge temporary construction facilities and result in large expenses and work time (Fig. 1).

If damage can be made occur at a part where recovery work can be easily done (Fig. 2), more reasonable aseismic design of RC pier structure according to construction conditions including recoverability can be achieved.

In this study, we carried out a static cyclic loading test using RC pier specimens with a high ratio of calculated shear capacity to flexural capacity and investigated the damage modes based on

the points where longitudinal rebars first yielded or broke. In this report, we cover the damage state of each damage mode and the classification of damage modes. We classified damage modes by the anchorage length of the cut-off rebars above section 1D (D = section height) and the bending performance (the ratio between the flexural capacity calculated only on the non-cut rebars at the rebar cut-off point and the bending moment that occurs at the rebar when flexural capacity occurs at the base).

### 2 Outline of Loading Test

Fig. 3 shows the reinforcement arrangement and a shape of the specimens, and Table 1 lists the specimen specifications. Assuming a usual RC pier of a railway structure, we set the cross-sectional dimensions to be approx. 1/3 to 1/5 those of an actual pier. The amount of the longitudinal rebars of the specimens is changed at the middle of their frames. One of the parameters set for the specimens is the ratio between the bending moment that acts at the cut-off point where the amount of the longitudinal rebars changes and cross-sectional performance in relation to bending that is calculated only on the non-cut rebars ("bending yield strength", or "flexural capacity"). We hereafter call that ratio the "flexural performance ratio at bending yield" or "flexural performance ratio in relation to flexural capacity" (Fig. 3 right). Another parameter is the ratio between the rebar length from the position of the cross-section height above the base of the specimen ("1D position") to the rebar and the rebar diameter ("anchorage length above 1D"). And the final parameter is the ratio of calculated shear capacity to flexural capacity at the base of the specimen and above the rebar cut-off point ("strength ratio"). Past studies clarified that damage area at the pier base is largely focused on the 1D section when damage occurs first at the base. With cut-off rebars, however, the length of rebars out of the damage area at the base would be the anchorage. We thus included the anchorage length above 1D in the parameters.

As bond deterioration of cut-off rebars occurs at the end of tension reinforcement, the current design standard<sup>1)</sup> defines the

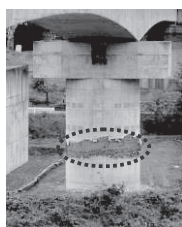


Photo 1 Example of Damage at Cut-off

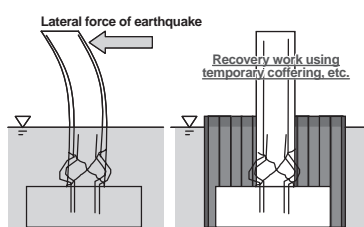


Fig. 1 Recovery after the Damage at the Base

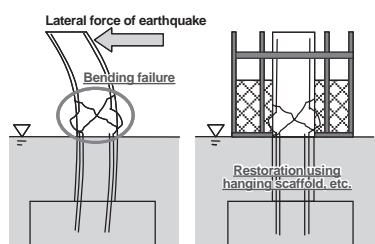


Fig. 2 Example of Recovery after Damage at the Intermediate Part of the Pier

Table 1 Specimen Specifications

Specimen	Height of cut-off (mm)	Anchorage length above 1D ( $\emptyset$ )	Longitudinal rebar arrangement			Ratio of tensile rebar (at cut-off) $P_{tc}$	Ratio of tensile rebar (at base) $P_{tb}$	Ratio of calculated shear capacity to flexural capacity		Flexural performance ratio	Flexural performance ratio	Tie hoop interval (mm)	Longitudinal force (MPa)
			Net cover concrete	Cut-off	Base			Cut-off	Base				
D-9	1150	80	31mm	d13 $\times$ 14	d13 $\times$ 20 in 2 layers	0.0024	0.0069	2.6	3.3	1.18	1.14	75	0.7
D-11	1200	85	30mm	d10 $\times$ 16	d10 $\times$ 22 in 2 layers	0.0031	0.0085	2.1	2.6	1.09	1.06	150	0.5
D-12	1280	93	30mm	d10 $\times$ 10	d10 $\times$ 18 in 2 layers	0.0019	0.0070	2.3	2.8	1.05	1.04	150	0.6
D-13	1470	112	30mm	d10 $\times$ 10	d10 $\times$ 24 in 2 layers	0.0019	0.0093	1.8	2.3	1.04	1.05	120	0.6
D-15	1240	89	30mm	d10 $\times$ 15	d10 $\times$ 21 in 2 layers	0.0029	0.0082	2.0	2.6	1.15	1.13	150	0.6
D-18	680	21	32mm	d16 $\times$ 30	d16 $\times$ 35, d16 $\times$ 9	0.0029	0.0082	1.8	2.6	1.11	1.08	80	0.6
D-19	1090	74	30mm	d10 $\times$ 30	d10 $\times$ 38 in 2 layers	0.0029	0.0074	2.2	2.6	1.06	1.00	120	0.6
D-20	1170	82	30mm	d10 $\times$ 27	d10 $\times$ 38 in 2 layers	0.0026	0.0074	2.2	2.6	1.06	1.00	120	0.6
D-21	680	25	29mm	d13 $\times$ 26	d13 $\times$ 33, d13 $\times$ 7	0.0046	0.0071	2.2	2.4	1.06	1.04	120	0.6
D-23	1000	65	30mm	d10 $\times$ 19	d10 $\times$ 25 in 2 layers	0.0037	0.0097	2.4	2.5	0.96	0.93	120	0.7

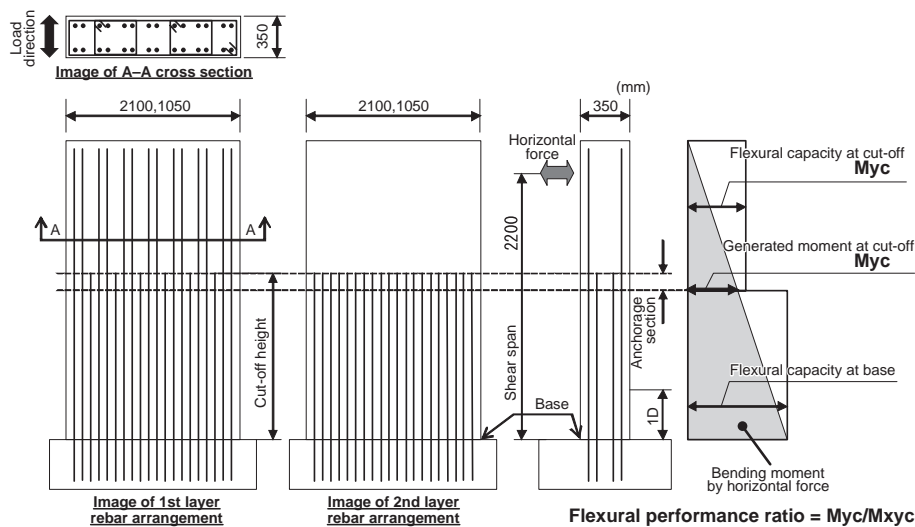


Fig. 3 Specimen Overview

position under the rebar cut-off point by the anchorage length of the main reinforcement as “cut-off”. If stress repeatedly acts at the end of the cut off rebars, it is difficult to accurately identify the length of the bond deterioration of the rebars. Thus, we set the parameters for the specimens using the rebar cut-off point as the base point.

The rebar cut-off points of the specimens are located within the range between 1/3.2 and 1/1.5 of the shear span. In this condition, the flexural performance ratio at the rebar cut-off point at the bending yield is between 0.96 and 1.18. The ratio of calculated shear capacity to flexural capacity of the specimens is between 2.3 and 2.8 under the rebar cut-off point and between 1.8 and 2.6 above the rebar cut-off point. We avoided remarkable shear damage, based on the past studies<sup>2), 3)</sup>.

In the cyclic loading test, we defined as “yield displacement  $\delta_y$ ” the horizontal displacement of the load point at the point when the strain of the main reinforcement of the specimen base on the outermost edge in the loading direction reached the yield strain. We applied loads, sequentially increasing the displacement amplitude by the integral multiple of horizontal displacement  $n \times \delta_y$  ( $n = 1, 2, 3, \dots, 12, 14, 16\delta_y$  after  $10\delta_y$ ).

### 3 Outline of Cyclic Loading Test Results

#### 3.1 Classification of Damage Modes

Through the test results, we classified the damage modes by the position where the longitudinal rebars yielded and the position where the load bearing ability was lost due to excessive damage. The progress of damage in tests per damage mode is as follows.

##### (1) Damage mode 1: Base yield and base failure

Specimen D-15 was a specimen with which the longitudinal rebars yielded at the base and then the base failed. This mode of failure is often seen in experiments with columns and the like. Fig. 4 shows the cracking of D-15 at some of the load application steps.

The flexural performance ratio at bending yield at the rebar cut-off point of D-15 was 1.15. Cracks on its concrete surfaces were generated upward from the base to a height around 20 times the longitudinal rebar diameter above the rebar cut-off point. The longitudinal rebars reached yield strain at the base.

From  $2\delta_y$  to a maximum loading of  $6\delta_y$ , expansion of the crack width was observed at the rebar cut-off point and the base. Near the rebar cut-off point, only the cracks at the rebar cut-off point expanded remarkably. The crack width at maximum horizontal displacement in the  $6\delta_y$  loading step was approx. 3.0 mm at the rebar cut-off point and approx. 2.5 mm at the base.

With hammering tests at the maximum horizontal

displacement in the 7 $\delta y$  loading step, peeling was found on the cover concrete. The area of the peeling was approx. five times longer than the longitudinal rebar diameter downward from the rebar cut-off point and approx. 40 times longer than that upward from the upper surface of the footing at the base. In the 8 $\delta y$  loading step caused crushing at the base, significantly lowering the horizontal load. Photo 2 shows the specimen at the end of the test.

## (2) Damage mode 2: Base yield and flexural failure near the rebar cut-off point

Specimen D-19 was a specimen with which the longitudinal rebars yielded at the base and failure occurred near the rebar cut-off point. Fig. 5 shows the cracking of D-19 at some of the load application steps.

The flexural performance ratio at bending yield at the rebar cut-off point of D-19 was 1.06. With 5 $\delta y$  loading, remarkable concentration of cracks around the rebar cut-off point was observed and crushing was found. At that time, peeling of the cover concrete occurred in the area approx. five times lower than the longitudinal rebar below the rebar cut-off point. With 7 $\delta y$  loading, crushing advanced near the rebar cut-off point. With 9 $\delta y$  loading, spalling of the cover concrete became remarkable, exposing the longitudinal rebars. Photo 3 shows D-19 at the end of the test.

## (3) Damage mode 3: Yield and failure near the rebar cut-off point

Specimen D-12 was a specimen with which the longitudinal rebars yielded near the rebar cut-off point. Then the specimen failed near the rebar cut-off point. Fig. 6 shows the cracking of D-12 at some of the load application steps.

The flexural performance ratio at bending yield at the rebar cut-off point of D-12 was 1.05. With 5 $\delta y$  loading, peeling of the cover concrete was found in the area from the point by approx. three times lower than the longitudinal rebar diameter below the rebar cut-off point to the point by approx. five times higher than the same above the rebar cut-off point. With 6 $\delta y$  loading, the longitudinal rebars buckled near the rebar cut-off point, causing spalling of the cover concrete. The area of the spalling was around 17 times longer than the longitudinal rebar diameter. Photo 4 shows D-12 at the end of the test.

## (4) Damage mode 4: Base yield, combination of bond deterioration of the cut-off rebars above 1D and base failure

Specimen D-18 was a specimen with which the anchorage length above 1D was 21 times longer than the longitudinal rebar diameter. Fig. 7 shows the cracking of D-18 at some of the loading steps.

With D-18, the longitudinal rebars yielded at the base. The largest width of the cracks was found at the base at yielding. With 2 $\delta y$  loading, the cracks around the rebar cut-off point greatly expanded, and cracks occurred along the longitudinal rebars in the longitudinal direction of members in the area from the base to the rebar cut-off point. From the rebar cut-off point, many short cracks occurred diagonal to the base. Above the rebar cut-

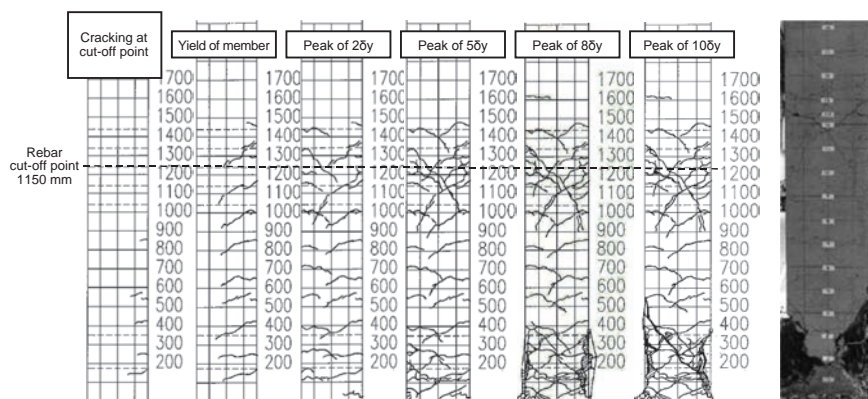


Fig. 4 Damage of Specimen D-15

Photo 2

D-15 at the End of Test

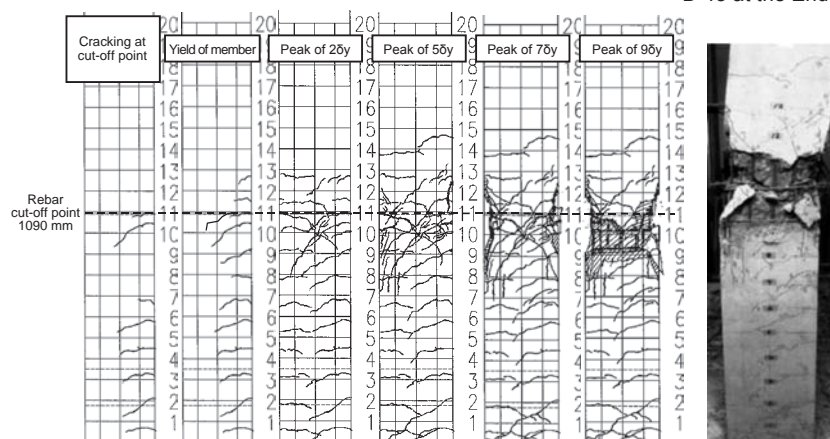


Fig. 5 Damage of Specimen D-19

Photo 3

D-19 at the End of Test

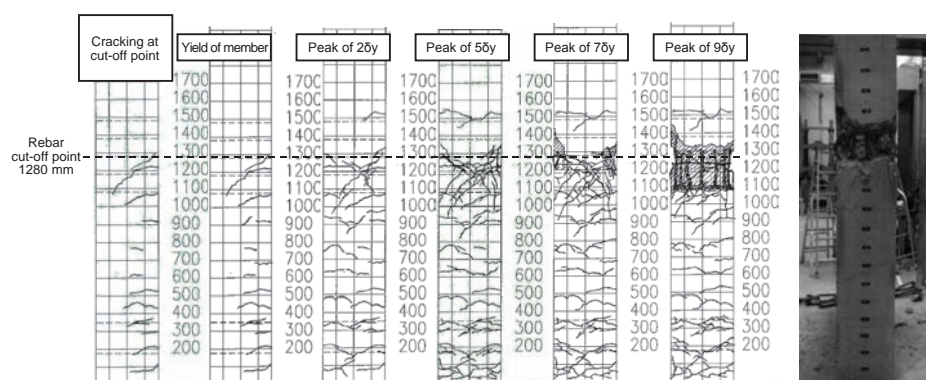


Fig. 6 Damage of Specimen D-12

Photo 4

D-12 at the End of Test

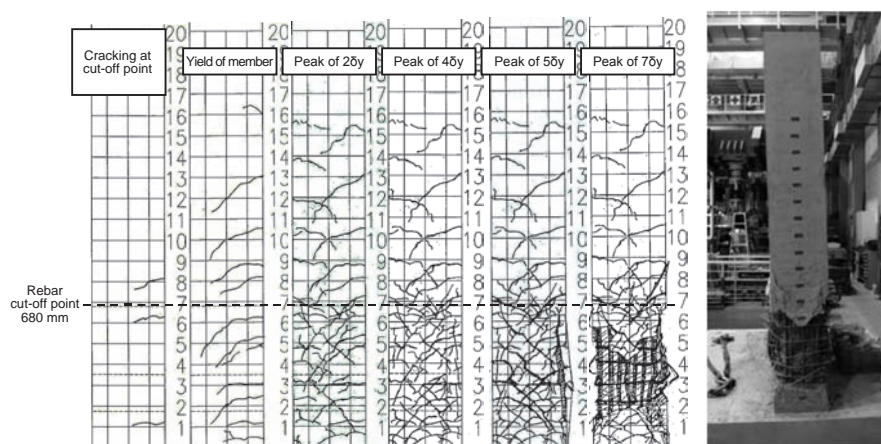


Fig. 7 Damage of Specimen D-18

Photo 5

D-18 at the End of Test

off point, almost no increase or advance of cracks was found.

With the  $5\delta_y$  loading step, the cover concrete was crushed and the longitudinal rebars buckled in the area from the base to the rebar cut-off point, but no buckling of the cut-off rebars was found. Spalling of the cover concrete to near the rebar cut-off point would indicate that this is because anchorage was lost above 1D.

The area of the spalling of the cover concrete was from the base to the rebar cut-off point. Thus, the damage to D-18 is assumed to be compound damage of crushing of the base concrete, buckling of non-cut rebars and bond deterioration of cut-off rebars above 1D. Photo 5 shows D-18 at the end of the test.

### 3.2 Distribution of Strain of Longitudinal Rebars

Here we describe the distribution of strain of the longitudinal rebars of specimens D-15 and D-19. In cyclic loading tests, the base yielded first and then was crushed with D-15. The base yielded first, then damage shifted to near the rebar cut-off point and the specimen failed there with D-19.

Fig. 8 shows the distribution of strain of the non-cut rebars and cut-off rebars of specimen D-15. The strain of the longitudinal rebars with up to  $7\delta_y$  loading was a little larger at the rebar cut-off point than at the base. Under  $8\delta_y$  loading, the strain of the rebars near the base exceeded that of the rebars near the rebar cut-off point. Under  $9\delta_y$  loading, the rebars buckled at

the base. In D-15, strain of the rebars did not increase so much as load increased, even though the non-cut rebars yielded near the rebar cut-off point.

Fig. 9 shows the distribution of strain of D-19 under which yielding occurred first at the base and then failure occurred at the rebar cut-off point. In D-19, we found expansion of the area of rebar yielding at the base in  $2\delta_y$  to  $4\delta_y$  loading. From  $4\delta_y$  loading, strain of the non-cut rebars near the rebar cut-off point exceeded that at the base. Under  $6\delta_y$  loading, the non-cut rebars near the rebar cut-off point started buckling. With D-19, the non-cut rebars near the rebar cut-off point yielded and a tendency for strain of the rebars there to be accumulated as the load increased was observed.

## 4 Study of Mechanism where Yield Occurs First at the Base and Damage Shifts to the Rebar Cut-off Point

Specimen D-19 yielded at its base and damage shifted to around the rebar cut-off point before it failed. D-13 also showed a form of damage similar to that of D-19. Thus, based on the position of yielding, we investigated the damage mechanism where damage shifted to around the rebar cut-off point using distribution of the strain of the rebars. According to the shift of the strain of the rebars, the mechanism of the shift of damage can be presumed as follows.

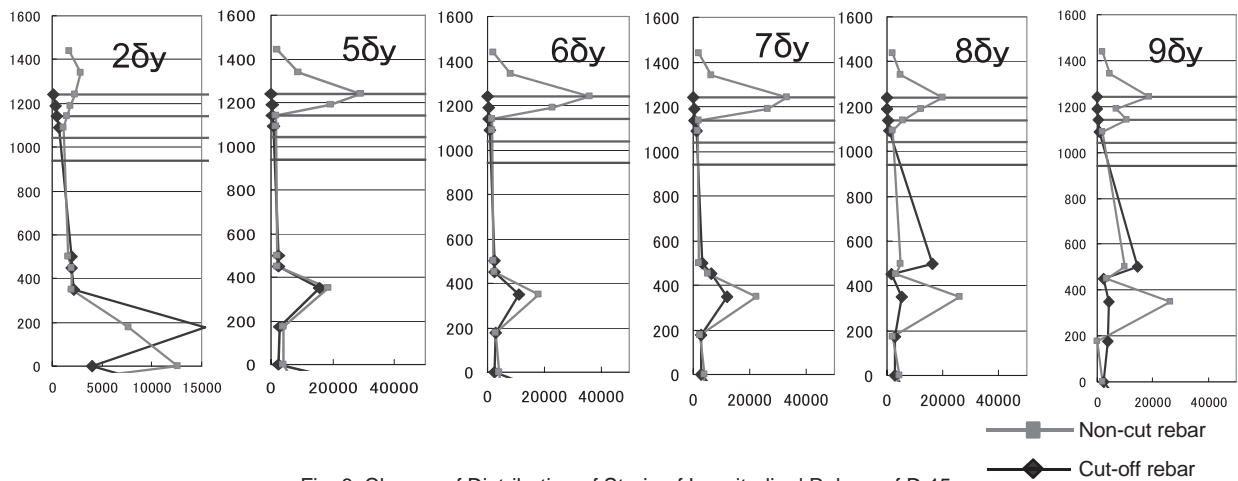


Fig. 8 Change of Distribution of Strain of Longitudinal Rebars of D-15

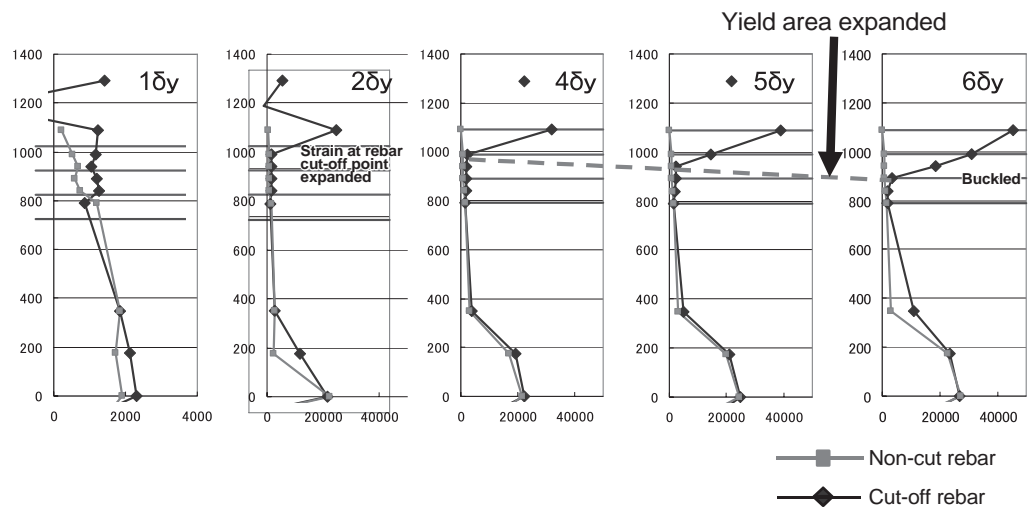


Fig. 9 Change of Distribution of Strain on Longitudinal Rebars of D-19

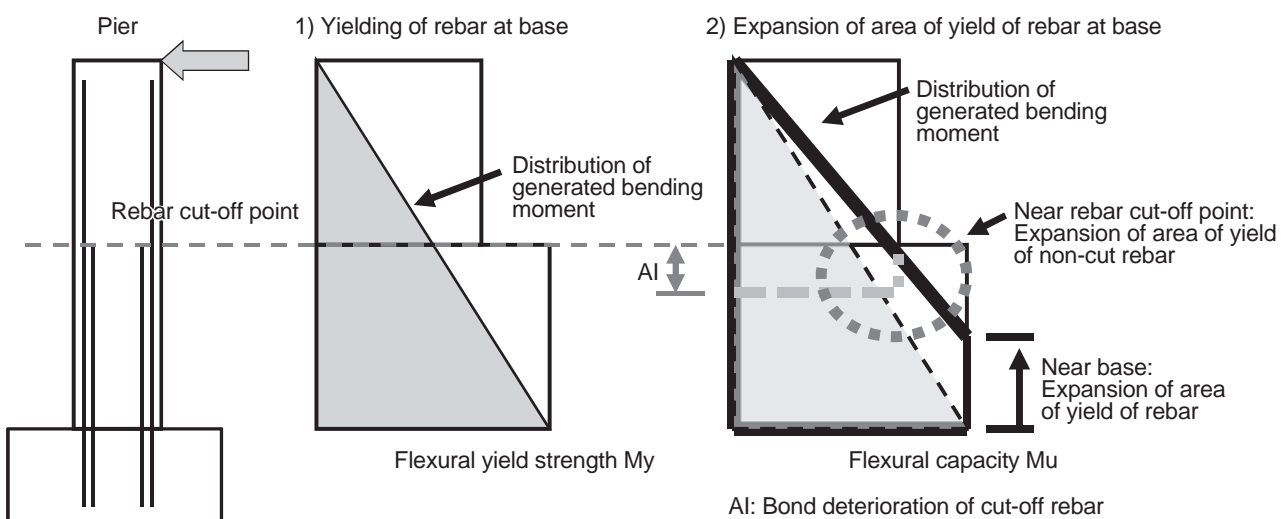


Fig. 10 Mechanism of Damage Shift to Rebar Cut-off Point after Base Yield

- 1) At the early stage of loading, the area of the yield of the rebars expands.
- 2) The expansion of the yield area of the rebars changes the distribution of the bending moment as seen in Fig. 10.
- 3) As in Fig. 10, the distribution of the generated bending moment

changes, the generated bending moment increases near the rebar cut-off point, and the area of the bond deterioration of the cut-off rebars expands. The expansion of the yield area of the non-cut rebars and the generated strain of the rebars near the rebar cut-off point are more prominent than those at the base.

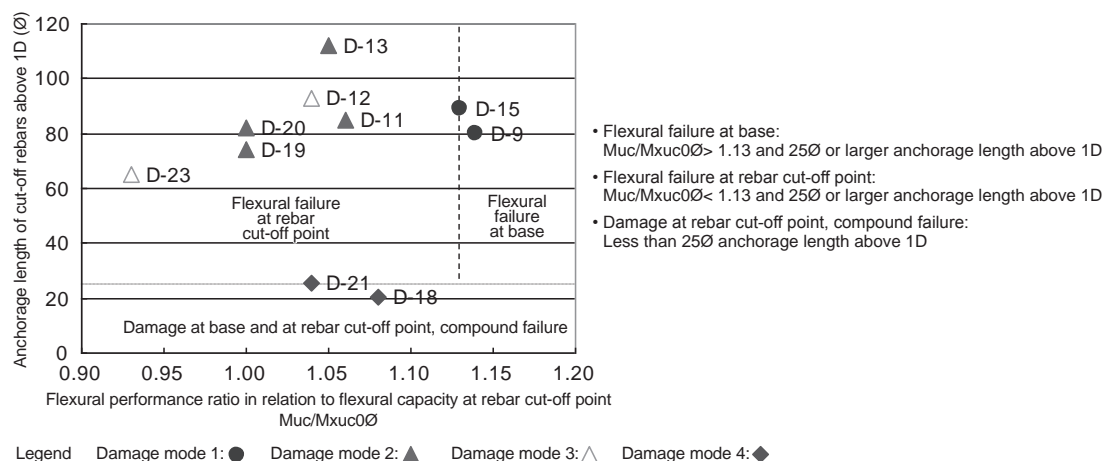


Fig. 11 Classification Map of Part where Flexural Damage Occurred with RC Piers having Cut-off Rebars

4) The rebars near the rebar cut-off point starts buckling. That causes spalling of the cover concrete, advances damage near the rebar cut-off point and finally results in failure.

As the yield area of the rebars at the base expands, the generated bending moment shifts. The test results demonstrated that the damage shifted and failure occurred near the rebar cut-off point when the flexural performance ratio at flexural capacity at the rebar cut-off point was between 1.05 and 1.15.

## 5 Study on Method of Identifying Where Failure Occurs

Based on the cyclic loading test results, we studied a method of identifying where failure occurs on RC piers with cut-off rebars.

With the specimens used in the cyclic loading tests, the rebar cut-off point was located in an area between  $1/3.2$  and  $1/1.5$  of the shear span. The flexural performance ratio at bending yield at the rebar cut-off point was between 0.96 and 1.20, and the ratio of calculated shear capacity to flexural capacity was between 2.3 and 2.8 below the rebar cut-off point and between 1.8 and 2.6 above that point. Shear damage was not predominant at those locations.

Assuming such specifications, the most decisive parameters on where failure occurs with the specimens should be the anchorage length above  $1D$  and the flexural performance ratio at the rebar cut-off point in relation to flexural capacity. Fig. 11 shows the flexural performance ratio in relation to flexural capacity on the X-axis and the anchorage length of the cut-off rebars above  $1D$  on the Y-axis. We believe that we can, for the most part, identify where failure occurs with RC piers having cut-off rebars where flexural damage is prominent.

## 6 Conclusion

We studied flexural damage of RC piers having cut-off rebars through cyclic loading tests using model specimens. The study results are as follows.

(1) With specimens having flexural performance ratio of 1.13 or larger at the rebar cut-off point in relation to flexural capacity, the base first yielded and then flexural failure occurred that

point.

- (2) With specimens having a flexural performance ratio of around 1.0 at the rebar cut-off point in relation to flexural capacity, the base first yielded, damage then shifted to near the rebar cut-off point, and finally flexural failure occurred near the rebar cut-off point.
- (3) The reason why yield of the rebars first occurred at the base and damage then shifted to the rebar cut-off point was that expansion of the area of rebar yield at the base shifted the generated bending moment. As the generated bending moment near the rebar cut-off point increased, damage consequently shifted from the base to the rebar cut-off point.
- (4) With specimens having a flexural performance ratio of between 0.96 and 1.03 at the rebar cut-off point, first yield and then flexural failure occurred at the rebar cut-off point.
- (5) With specimens having an anchorage length of  $25\phi$  or less for cut-off rebars above  $1D$ , yield first occurred at the base, and then a combination of bond deterioration of cut-off rebars above  $1D$  and failure at the base occurred.
- (6) Within the specifications of the specimens used, we can for the most part identify where damage occurs according to the anchorage length of the cut-off rebars above  $1D$  and the flexural performance ratio at the rebar cut-off point in relation to flexural capacity.

### Reference:

- 1) Railway Technical Research Institute, comp., Railway Bureau, Ministry of Land, Infrastructure, Transport and Tourism, edit., *Design Standards for Railway Structures and Commentary (Concrete Structures)*, Maruzen Company Limited (April 2004)
- 2) Tadayoshi Ishibashi, Takeshi Tsuyoshi, Kaoru Kobayashi, Masashi Kobayashi, "An Experimental Study on Damage Levels and Repairing Effects of Reinforced Concrete Columns Subjected to Reversal Cyclic Loading with Large Deformations," Japan Society of Civil Engineers, *Journal of Materials, Concrete Structures and Pavements*, Vol.47, No. 648 (May 2000): 55–69
- 3) Hisako Kobayashi, Shigehiko Saito, Koichiro Ota, Kaoru Kobayashi, "RC Kyokuyaku Dan-otoshi-bu no Mage-sonsho Mechanism ni kansuru Kisoteki Kenkyu [in Japanese]," *Proceedings of Annual Conference of the Japan Society of Civil Engineers* Vol. 32, No. 2 (2010): 19–24